Numerical Simulation of the Impact of Smoke Management Scenarios on Visibility in a Car Park

Ghodrat Ghassabi *[1], Mahmood Moghddam [2], Seyed Sajad Noorbakhsh [1], Farhad Yeganeh [1]

[1] Department of Mechanical Engineering, Faculty of Engineering, Bozorgmehr University of Qenat, Qaen, Iran
[2] Arman Tahviye Sanabad Company, Mashhad, Iran

ABSTRACT: The mechanical ventilation smoke management system involves the use of supply fans, jet fans, and exhaust fans, which are activated at different times after a fire is extinguished. This paper numerically investigates the effect of the priority and delay of smoke management systems on smoke distribution and visibility in a car park after a fire, using Fire Dynamic Simulation Code 6.7.6. The flow rates of the exhaust fan, supply fan, and jet fan are 1.9 m³/s, 1.43 m³/s, and 1.67 m³/s, respectively. The fire, located near the supply fans, is modeled as a rectangle with dimensions of 2.0×0.8 m² and a power of 1.6 MW, lasting for one minute from ignition to extinguishment. Polyurethane is assumed as a flammable material. The priority and delay of the smoke management systems are evaluated through four scenarios over a period of 420 seconds. The results show that visibility reaches acceptable levels in all scenarios at all locations after 420 seconds. Additionally, the results indicate that the visibility of the upper half is highest for scenario a, at around 15 m. However, the visibility of the lower half is highest for scenario d, ranging between 20 and 30 m. It can be concluded that delaying the activation of smoke management systems is an effective strategy for facilitating smoke removal and fresh air intake.

1- Introduction

In closed parking lots where natural ventilation is not feasible, mechanical ventilation becomes essential. To address this, the Iran Fire Department has established regulations titled "Regulations and Criteria for Ventilation, Exhaust, and Smoke Control Systems." These regulations mandate that all buildings with three or more underground floors, or with a gross area exceeding 500 square meters per underground floor, comply with the directive. The calculation, design, and positioning of the smoke management system, along with the evaluation of activation scenarios, are the responsibility of HVAC design companies. Iran Fire Department typically approves the completion of work on closed parking lots and larger complexes after reviewing the smoke management system, and the smoke scenario, and sometimes after studying the computational fluid dynamics (CFD) simulation of smoke movement using Fire Dynamics Simulator (FDS) code 6.7.6. Therefore, extensive research has been conducted in this field. Liao et al. [1] simulated the smoke exhaust flow in the underground city of Guangzhou using PyroSim software. Their results show that the temperature at the end of both main passages increases faster, so their evacuation time decreases, and it takes only 143 seconds to evacuate. Zhou et al. [2] modeled a college building in PyroSim software.

This educational building has two floors with an area of 6380 m², with 3 staircases and 4 emergency exits. The simulation results indicate that smoke reached the critical height in stairwells 1 and 2 on the second floor in 63 seconds and 76 seconds, respectively. Despite the relatively large distance from the fire classroom, smoke reached the critical height in stairwell 3 on the second floor in 123 seconds, making the stairwell impassable. Their results also showed that the total evacuation time increased by up to 21 seconds after the fire. Long et al. [3] numerically simulated a dormitory fire and the evacuation of people using PyroSim and Pathfinder software. The simulation results showed that when the window is open, smoke first exits through the window and then spreads upwards. When the window is closed, smoke exits through the door and spreads upwards through the stairwell. The results indicate that it is preferable to keep the window of the fire room open while keeping the windows of the upper floors closed. The lowest visibility, approximately 5 m, was observed on the left side of the second floor. Zhou et.al [4] numerically investigated the smoke exhaust effect using both the whole region and sub-region modes. Their results show that the visibility and temperature decrease faster in whole region mode. Wang et al. [5] numerically studied the smoke spread in the stairwell of an apartment. This study considered the chimney effect due to buoyancy forces in the stairwell. Their results indicated that the carbon monoxide

*Corresponding author's email: Ghodrat.ghassabi@buqaen.ac.ir

concentration reached 200 ppm on the ground floor after 4 minutes. Kemkova et al. [6] designed a smoke management system for an underground car park using jet fans. Their simulation results demonstrated that the placement of the exhaust fans was appropriate, and the smoke was exhausted after 1300 seconds. They also observed that the visibility range after 1300 seconds from the fire was 25 m to 30 m. Yuan et al. [7] simulated smoke control in a large enclosure in Stockholm using natural ventilation and smoke curtains. The enclosure was 39 m long, 11 m wide, and 8 m high. The smoke curtain acted as a physical barrier to prevent smoke from spreading from one area to another. This curtain created a highly pressurized region, causing the smoke to exit the outlets at a higher velocity. It was observed that using a 2 m smoke curtain delayed the smoke spread to the other part of the enclosure by approximately 120 seconds. It was observed that the smoke spread was completely contained, for 4 m and 6 m smoke curtains. Hakimzade and Talaee [8] simulated tunnel fire ventilation using a fire dynamics simulator. They investigated the effect of delay in emergency ventilation on the distribution of fire products. The results indicate that a delay in emergency ventilation leads to the dispersion of fire products within the tunnel, posing a threat to passengers as they navigate an unsafe escape route during a fire upstream after the system is activated. Wang et al. [9] numerically simulated the natural smoke flow in a tall and narrow atrium. Their results show that the vertical velocity gradually decreases with increasing height, and the smoke flow creates a larger cross-sectional area at higher elevations. Behbahani et al. [10] simulated a car park in a commercial building, investigating three different scenarios. In these scenarios, the effects of ventilation and a jet fan on visibility and temperature were studied. Results show that temperature decreases by 44.1% while the visibility increases by 15.59 times using ventilation and a jet fan. Wong et al. [11] numerically investigated the effect of the dimensions and location of exhaust fans in an office space. Their results showed that changing the dimensions of the exhaust fans has no significant effect on the smoke layer height. However, the placement of the fans on the upper part of the wall is highly influential. Nguyen and Boo [12] conducted a transient numerical simulation of smoke flow in an environment with dimensions of $30 \times 20 \times 4$ m^3. Their results showed that for heights less than 1.4 m, the temperature is below 65 ^{0}C, and the visibility field is 10 m. Li et al. [13] simulated the fire and evacuation of people using PyroSim and Pathfinder software in a public underground space. Their results indicated that out of 718 people, 552 were able to evacuate before the stairs became unstable.

The mechanical ventilation smoke management system includes supply fans, jet fans, and exhaust fans, which are activated at different times after a fire is extinguished to facilitate ventilation and smoke exhaust from the parking lot. The timing and sequence for activating this mechanical ventilation equipment, known as the "smoke management scenario," are not specified in Iran fire department regulations and are still reviewed and approved on a case-by-case basis.

Moreover, Researchers have not conducted significant studies on the impact of smoke management scenarios on the visibility and temperature distribution of car parking.

In this research, the effect of the sequence and timing of smoke management systems on accelerating smoke exhaust after a fire was investigated by creating the geometry of a car park equipped with a smoke management system in PyroSim software. The boundary conditions and required flow rates for the smoke management systems were based on fire department standards. The parking environment was meshed, and simulations were performed for different scenarios of the smoke management system, focusing on the priority of equipment activation and its effect on visibility fields and velocity distribution.

2- Simulation, Boundary Condition

In Fig. 1, the plan view of the parking lot under study is presented, showing the dimensions and location of the supply air vents (left side, blue duct, and vents), jet fans (middle section), and exhaust air vents (right side, orange duct, and vents). This smoke management system consists of 6 exhaust vents, 4 jet fans, and 4 supply vents. The flow rate of the smoke management system is determined according to the fire department regulations, based on 10 air changes per hour for the exhaust fans and 50% of this amount for the supply vents in the event of a fire[14]. As a result, each exhaust vent has a flow rate of 1.9 m³/s, as defined by the exhaust fan boundary condition in PyroSim software. Tthe supply vent flow rate is 1.43 m³/s, defined by the intake fan boundary condition in PyroSim software and the jet fans have a flow rate of 1.67 m³/s. The red rectangle with dimensions of 2.0×0.8 m² indicates the location of the 1.6 MW fire, which is considered to last one minute from ignition until extinguishment, as defined by the constant heat flux boundary condition in PyroSim software. The polyurethane, represented by the formula $C_3H_8N_2O$, is assumed to be the flammable material [14].

3- Governing Equations and Mathematical Model

Based on the flow state and flow rate value, the flow regime is turbulent. Therefore, the governing equations are as follows [15]:

Continuity:

$$\frac{\partial \rho}{\partial t} + \frac{\partial}{\partial x}(\rho \bar{u}) + \frac{\partial}{\partial y}(\rho \bar{v}) + \frac{\partial}{\partial z}(\rho \bar{w}) = 0 \tag{1}$$

x- Momentum:

$$\rho \frac{d\bar{u}}{dt} = -\frac{\partial \bar{p}}{\partial x} + \frac{\partial}{\partial x}(\mu \frac{\partial \bar{u}}{\partial x} - \rho \overline{u'^2})$$
$$+ \frac{\partial}{\partial y}(\mu \frac{\partial \bar{u}}{\partial y} - \rho \overline{u'v'}) + \frac{\partial}{\partial z}(\mu \frac{\partial \bar{u}}{\partial z} - \rho \overline{u'w'}) \tag{2}$$
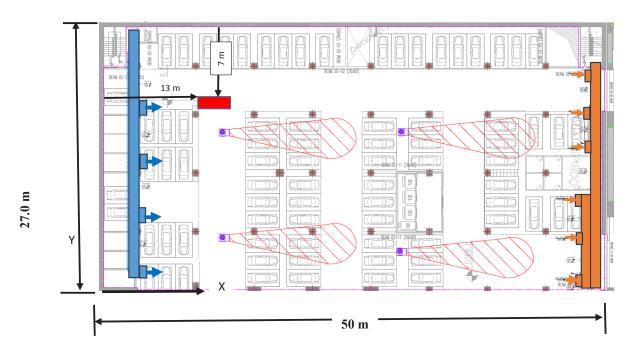
Fig. 1. Plan view of the parking lot under study, showing the dimensions and locations of the exhaust ducts (left side), jet fans (middle section), and supply ducts (right side)

y- Momentum:

$$\rho \frac{d\bar{v}}{dt} = -\frac{\partial \bar{p}}{\partial y} + \frac{\partial}{\partial x}(\mu \frac{\partial \bar{v}}{\partial x} - \rho \overline{u'v'})$$
$$+\frac{\partial}{\partial y}(\mu \frac{\partial \bar{v}}{\partial y} - \rho \overline{v'^2}) + \frac{\partial}{\partial z}(\mu \frac{\partial \bar{v}}{\partial z} - \rho \overline{v'w'})$$

(3)

z- Momentum:

$$\rho \frac{d\bar{w}}{dt} = -\frac{\partial \bar{p}}{\partial z} + \frac{\partial}{\partial x}(\mu \frac{\partial \bar{w}}{\partial x} - \rho \overline{u'w'})$$
$$+\frac{\partial}{\partial y}(\mu \frac{\partial \bar{w}}{\partial y} - \rho \overline{v'w'}) + \frac{\partial}{\partial z}(\mu \frac{\partial \bar{w}}{\partial z} - \rho \overline{w'^2})$$

(4)

Energy:

$$\frac{d\bar{T}}{\partial t} = \frac{\partial}{\partial x}(\alpha \frac{\partial \bar{T}}{\partial x} - \overline{u'T'}) + \frac{\partial}{\partial y}(\alpha \frac{\partial \bar{T}}{\partial y} - \overline{v'T'})$$
$$+\frac{\partial}{\partial z}(\alpha \frac{\partial \bar{T}}{\partial z} - \overline{w'T'}) + q_r$$

(5)

where is the air density, t is the time, $\vec{V}$ is the velocity

vector, *u*, *v*, and *w* are the velocity components in the *x, y,* and *z* direction, *p* is the pressure, *T* is the temperature, μ is the kinematic viscosity, α is the thermal diffusivity and q_r is a source term due to the heat release of the fire.

To model turbulence, the standard k-ε model was employed, which focuses on the processes affecting kinetic turbulent energy. This model involves solving two transport equations to calculate the kinetic energy (*k*) and turbulence dissipation (ε), as outlined below[16]:

$$\frac{\partial}{\partial t}(\rho k) + \frac{\partial}{\partial x_i}(\rho k u_i) =$$
$$\frac{\partial}{\partial x_i}\left[(\mu + \frac{\mu_t}{\sigma_k})\frac{\partial k}{\partial x_j}\right] + G_k + G_b - \rho \varepsilon - Y_m + S_k$$

(6)

$$\frac{\partial}{\partial t}(\rho \varepsilon) + \frac{\partial}{\partial x_i}(\rho \varepsilon u_i) =$$
$$\frac{\partial}{\partial x_i}\left[(\mu + \frac{\mu_t}{\sigma_\varepsilon})\frac{\partial \varepsilon}{\partial x_j}\right] + C_{1\varepsilon}\frac{\varepsilon}{k}(G_k + C_{3\varepsilon}G_b)$$
$$-C_{2\varepsilon}\rho\frac{\varepsilon^2}{k} + S_\varepsilon$$

(7)

In these equations, constant coefficients are as follows: $\alpha_\varepsilon = 0.72$, $C_\mu = 0.0845$, $\alpha_k = 0.72$, $C_{1\varepsilon} = 1.42$, and $C_{2\varepsilon} = 1.68$[16].

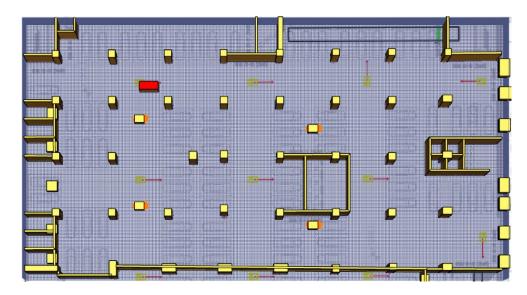**Fig. 2. Discretized computational domain of the parking garage modeled in the PyroSim software**
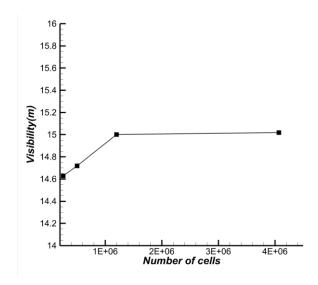

Fig. 3. Visibility value at x= 25 m and y =13.5 m for different numbers of grids

The parameters and equations above are presented in scalar form. The Arrhenius model is used to calculate the reaction rates due to the combustion of polyurethane. Fire Dynamics Simulation Code 6.7.6 and Pyrosim Software 2021 systematically solve the governing equations through discretization and computational fluid dynamics (CFD) numerical solution techniques. The governing equations are solved using a time step based on the flow speed within each specific mesh, allowing for time-dependent simulations of fire spread and smoke movement.

Fig. 2 shows the discretized computational domain of the parking garage. Fig.3 displays the visibility value at x= 25 m and y =13.5 m for different numbers of grids. It is shown that

the visibility value becomes constant for grids with 1,202,880 cells (cell size 0.15m) and 4,067,280 cells (cell size 0.1m). Therefore, to decrease the calculation time, a mesh consisting of cubic cells with dimensions of 15 cm per side has been applied for the detailed simulation of the smoke and airflow within the parking garage environment. This grid size is confirmed by with following equation, which describes the characteristic fire diameter [15].

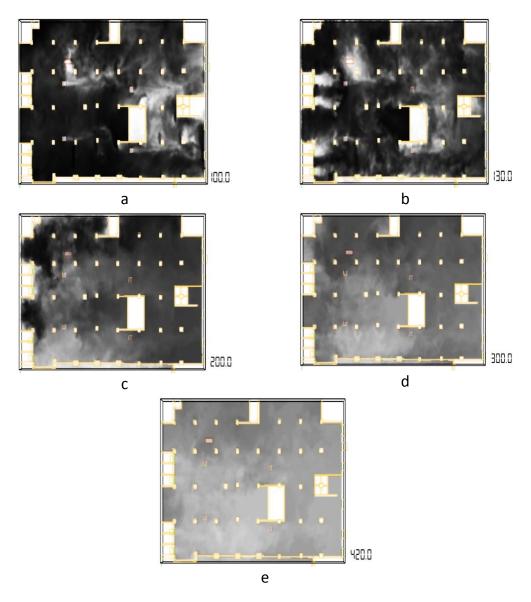$$D^* = (\frac{Q}{\rho_\infty C_P T_\infty \sqrt{g}})^{\frac{2}{5}} \tag{8}$$

Fig. 4. Smoke diffusion at different times (s)

In this equation, Q is the total heat release rate of the fire, p_∞ is the air density (kg/m³), c_p is the air-specific heat (kJ/kg. K), g is the gravitational constant (m/s²), T_∞ is the ambient temperature (K). Therefore, the value of D^* is 1.67 for this project. The D^*/dx ratio must be 4 for the coarse mesh, 10 for the medium one, and 16 for the fine (dx is the mesh size) [15]. For a medium mesh, the cell size should be 16 cm. Thus, a mesh size of 15 cm is a proper mesh size based on these criteria.

The smoke scenarios based on the cases approved by the fire department under different conditions are examined in this study, with the following cases:

a. Activation of the exhaust fan after 60 seconds, activation of the jet fan after 90 seconds, and activation of the supply fan after 120 seconds.

b. Simultaneous activation of the exhaust fan and jet fan after 60 seconds, followed by the activation of the supply fan after 90 seconds.

c. Activation of the exhaust fan after 60 seconds, followed by the simultaneous activation of the supply fan and jet fan after 90 seconds.

d. Activation of the exhaust fan after 60 seconds, activation of the supply fan after 90 seconds, and finally activation of the jet fan after 120 seconds.

4- Results

Fig. 4 shows the smoke diffusion at different time intervals. In Fig. 4(a), after 100 seconds, the smoke generated by the fire begins to diffuse toward the exhaust channels, and the smoke concentration gradually decreases due to the activation of the smoke management system. According to Fig. 4(c), after 200 seconds, the highest concentration
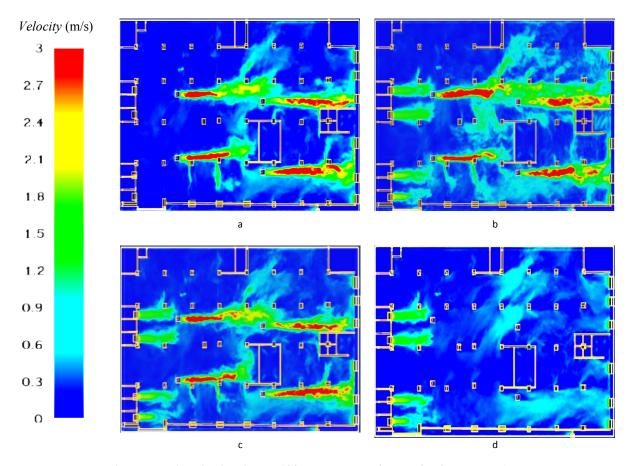
Fig. 5. Velocity distribution at 100 seconds at *z*=2.55 m for four scenarios

of smoke is in the left corner and in two corridors behind the supply ducts. Fig. 4(d) and 4(e) illustrate a significant decrease in smoke concentration. At 420 seconds, the smoke concentration is minimal, and all locations are clearly visible.

Fig. 5 shows the velocity distribution at 100 seconds at a height of *z*=2.55 m for four scenarios. By comparing Figs. 5(b) and 5(c) with Fig. 5(a), the results indicate that the supply ducts increase the air jet length of the two left-side jet fans. However, comparing Fig. 5(d) with the others reveals that the jet fan suction has no significant effect on the air jet supply. This is due to the design of the jet fans, where the suction direction is perpendicular to the supply air direction. Moreover, the scenarios do not significantly affect the air jet of the two right-side jet fans.

Fig. 6 presents the velocity distribution at 240 seconds at *z*=2.55 m for the four scenarios. It is observed that the jet fan located near the wall exhibits a lower velocity. Additionally, there is no significant difference in the velocity distributions between the scenarios.

Fig. 7 shows the visibility distribution at 240 seconds at *z*=1.95 m for the four scenarios. The results indicate that the upper left corner of the parking garage has the lowest visibility for all scenarios. This is due to the fire originating in that region, while the jet fans are located elsewhere. Furthermore, there is no significant difference in visibility between the scenarios in this area. According to Fig. 7, the highest visibility is in the lower left corner for all scenarios, as this corner is closest to the supply ducts and farthest from the fire. Additionally, visibility in scenario (d) is the highest in the lower left corner.

Fig. 8 shows the visibility distribution at 300 seconds at *z*=1.95 m for four scenarios. Similar to Fig.7, the results indicate that the upper left corner of the parking garage has the lowest visibility for all scenarios, with no significant difference between them in this area. Additionally, it can be observed that the lower left corner has the highest visibility for all scenarios. Furthermore, scenario (d) exhibits the highest visibility value in the lower left corner.

Fig. 9 presents the visibility distribution at 420 seconds at *z*=1.95 m for the four scenarios. It is observed that visibility reaches acceptable levels in all locations across all scenarios. Additionally, scenario (a) shows the highest
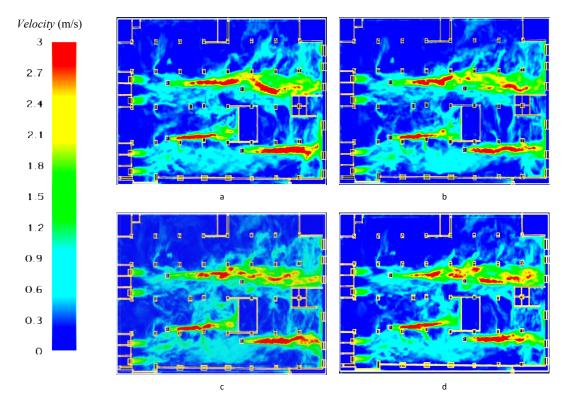
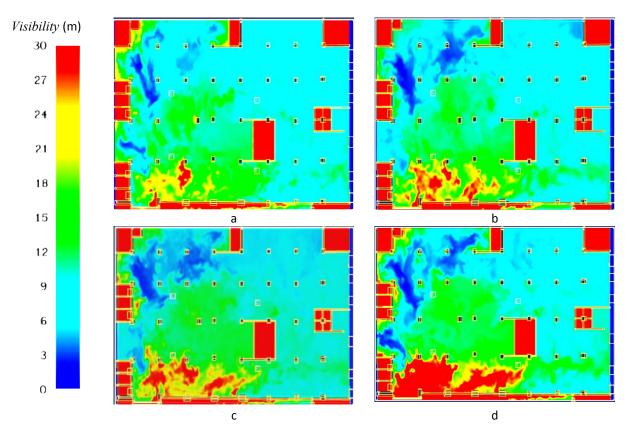**Fig. 6. Velocity distribution at 240 seconds at z=2.55 m for 4 scenarios.**

Fig. 7. Visibility distribution at 240 seconds at z=1.95 m for 4 scenarios
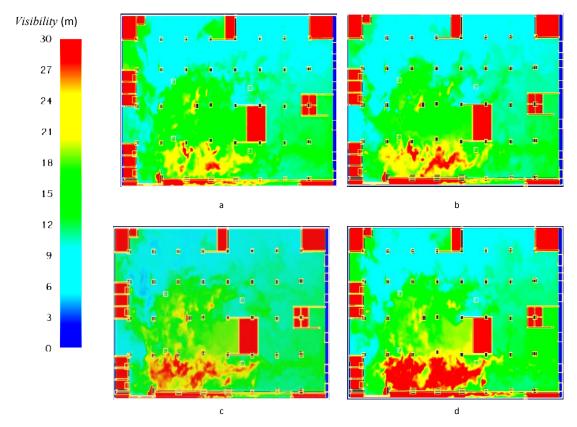
Fig. 8. Visibility distribution at 300 seconds at z=1.95 m for 4 scenarios
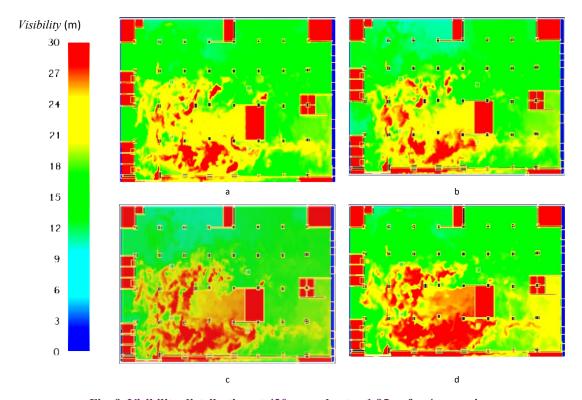

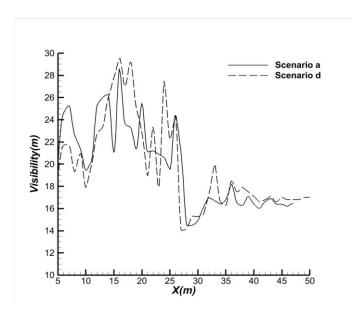**Fig. 9. Visibility distribution at 420 seconds at z=1.95 m for 4 scenarios**

Fig. 10. Visibility distribution in x-direction at 420 seconds at z=1.95 m and y=13.5 m for scenario a and d
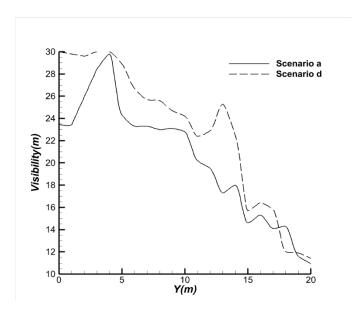

Fig. 11. Visibility distribution in y direction at 420 seconds at z=1.95 m and x=25 m for scenario a and d

visibility in the upper half, at around 15m. However, scenario (d) demonstrates the highest visibility in the lower half, and it is between 20 to 30m. Both scenarios (a) and (d) exhibit higher visibility values in the upper left corner (where the fire occurred) and it is around 15m. Therefore, there is no definitive best scenario for smoke management, but scenarios (a) and (d) perform better at reducing smoke concentration and increasing visibility. As a result, it can be concluded that introducing a delay between the activation of the smoke management systems is an effective strategy to facilitate smoke exit and the inflow of fresh air.

Fig. 10 illustrates the visibility distribution in the x-direction at $y = 13.5$ m and $z = 1.95$ m at 420 seconds for scenarios (a) and (d). It is evident that visibility fluctuates significantly due to the turbulence generated by the jet fan and the presence of obstacles. Furthermore, beyond $x = 25$ m, there is a noticeable reduction in visibility as the distance from the supply vents increases.

Fig. 11 presents the visibility distribution in the y-direction at $x = 25$ m and $z = 1.95$ m at 420 seconds for scenarios (a) and (d). The results indicate that visibility diminishes as a result of the fire being extinguished. Additionally, it is noteworthy that the visibility value is higher in scenario (d) compared to scenario (a).

5- Conclusion

In this paper, the effect of the order and timing of smoke management systems on smoke exhaust during a fire was numerically investigated using Fire Dynamic Simulation code 6.7.6. The boundary conditions and required flow rates for the smoke management systems were based on fire department standards. The following results were achieved:

Visibility reached reasonable levels for all scenarios in all locations after 420 seconds

Scenarios (a) and (d) showed higher visibility values in the upper left corner (the fire location).

There is no single best scenario for smoke management.

Scenarios (a) and (d) performed better in reducing smoke concentration and increasing visibility.

It can be concluded that introducing a delay between the activation of smoke management systems is an effective strategy to facilitate smoke exhaust and the inflow of fresh air.

References

[1] L. Liao, H. Li, P. Li, X. Bao, C. Hong, D. Wang, X. Xie, J. Fan, P. Wu, Underground Evacuation and Smoke Flow Simulation in Guangzhou International Financial City during Fire, Fire, 6(7) (2023) 266.

[2] M. Xu, D. Peng, PyroSim-Based Numerical Simulation of Fire Safety and Evacuation Behaviour of College Buildings, International Journal of Safety and Security Engineering, 10 (2020) 293-299.

[3] X. Long, X. Zhang, B. Lou, Numerical Simulation of Dormitory Building Fire and Personnel Escape Based on Pyrosim and Pathfinder, Journal of the Chinese Institute of Engineers, 40(3) (2017) 257-266.

[4] Y. Zhou, R.w. Bu, Z.s. Xu, H.j. Chen, J.h. Gong, Numerical Simulation of Smoke Control Effectiveness With Different Exhaust Modes In A Large Subway Station, Procedia Engineering, 211 (2018) 1065-1074.

[5] R. Wang, s. He, H. Yue, Numerical Study of Smoke Spread upon Shaft-box Type Double Skin Facades, Procedia Engineering, 211 (2018) 755-761.

[6] M. Kmecová, M. Krajčík, Z. Straková, Designing Jet Fan Ventilation for an Underground Car Park by CFD Simulations, Periodica Polytechnica Mechanical Engineering, 63(1) (2019) 39-43.

[7] A.C.Y. Yuen, T.B.Y. Chen, W. Yang, C. Wang, A. Li, G.H. Yeoh, Q.N. Chan, M.C. Chan, Natural Ventilated Smoke Control Simulation Case Study using Different Settings of Smoke Vents and Curtains in a Large Atrium, Fire, 2(1) (2019) 7.

[8] B. Hakimzadeh, M.R. Talaee, Analysis of Distribution of Toxic Species of a Fired Train in Ventilated Tunnel, Journal of Transportation Safety & Security, 13(7) (2019) 780-802.

[9] J. Wang, C. Du, H. Zhang, Numerical Simulation of Smoke Natural Filling in Ultra-Thin and Tall Atrium, Case Studies in Thermal Engineering, 28 (2021) 101.

[10] F. Behbahani, M. Hamzei, Z. Mehrdoost, M. Moghiman, Numerical Simulations on Visibility And Temperature in a Car Park of a Commercial Building, Journal of Manufacturing Engineering, 18(4) (2023) 141-144.

[11] Y. Wong, C. Voon Sia, K. Chong, M. Julaihi, A. Joseph, Numerical Study on the Smoke Movement in Office Rooms with Various Exhaust Vents Settings, Materials Today: Proceedings, 72(6) (2023) 2971-2977.

[12] T. Nguyen, H. Bui, Computational Fluid Dynamic Model for Smoke Control of Building Basement, Case Studies in Chemical and Environmental Engineering, 7 (2023) 100.

[13] X. Li, R. Chen, Y. Zhu, C.Y. Jim, Emergency Fire Evacuation Simulation of Underground Commercial Street, Simulation Modelling Practice and Theory, 134 (2024) 109.

[14] BS 7346-7, in: Components for smoke and heat control systems Part 7: Code of practice on functional recommendations and calculation methods for smoke and heat control systems for covered car parks, BSI Standards Publication, 2013.

[15] Fire Dynamics Simulator User's Guide, Fire Safety Research Institute, UL Research Institutes, Columbia, Maryland, 2024.

[16] B.S. Pope, Turbulence Flows, Cambridge University Press, United States of America, New York, 2007.